3D IN SITU CHARACTERISATION OF THE IMPREGNATION OF FIBROUS NETWORKS

Chiara Balbinot[1,2], Florian Martoïa[1], Laurent Orgéas[2], Pauline Carion[3], Frédéric Flin[4], Sabine Rolland du Roscoat[2], Jean-Francis Bloch[2], Maxime Terrien[3], Pierre J.J. Dumont[1]*

[1]Univ. Lyon, INSA-Lyon, CNRS UMR5259, LaMCoS, F-69621 Lyon, France
Email: chiara.balbinot@insa-lyon.fr; pierre.dumont@insa-lyon.fr
[2]Univ. Grenoble Alpes, CNRS, Grenoble INP, 3SR, UMR5519, F-38000 Grenoble, France
[3]Univ. Grenoble Alpes, CNRS, Grenoble INP, LGP2, UMR 5518, F-38000 Grenoble, France
[4]Météo-France, CNRS, CNRM, UMR 3589, CEN, F-38000, Grenoble, France

Keywords: Composite forming, impregnation, X-ray synchrotron microtomography, in situ characterisation, capillary effects, wettability.

Abstract
The control of the impregnation phase during the composite processes is crucial to obtain parts with optimised microstructures and end-use properties. The impregnation phase of the polymer matrix through the composite reinforcements can lead to the formation of voids and their deformation because of the effect of the matrix interstitial pressure, viscous and capillary effects. To understand the formation of voids, it is crucial to understand how the fluid front propagates within the reinforcements, at various scales and in particular within the fibre bundles. Therefore, in this study, X-ray microtomography was used to investigate the impregnation phenomena within model bundles. The 3D images obtained during in situ impregnation experiments allowed us to follow the evolution of the flow front position and shape as a function of the architecture of the fibre bundles, fluid viscosities and wettability conditions. Any variations in the architecture of the fibre bundle was shown to be responsible for slight variations in the capillary pressure, resulting in slight deformation of the geometry of the flow front.

1. Introduction

Owing to their outstanding specific physical and mechanical properties, fibre-reinforced polymer composites are increasingly used to make structural or multi-functional parts in the transportation and energy industries. An impregnation phase is usually needed for nearly all composite forming processes as evident for Liquid Composite Moulding processes [1, 2], but also for the fabrication of thermoformed or compression-moulded preimpregnated materials such as SMC [3, 4]. Impregnation consists of the flow of a polymer matrix through an anisotropic, deformable, and multiscale porous medium made of more or less ordered or disordered networks of fibre bundles, *i.e.*, arrays of aligned fibres. This phenomenon involves complex mechanisms, i.e., the permeation of the polymer matrices, capillary effects and the deformation of fibrous networks due to the fluid interstitial pressure, viscous and capillary effects, and also diffusion of the polymer matrix in the structure of porous fibres or fibre bundles, such as for example lignocellulosic fibres [5]. Besides, to enhance the mechanical properties of composites, extend their durability and/or to provide them functional properties, polymer matrices are often filled with mineral fillers, hollow beads with voids or self-healing resins, as well as high strength and slender nanofibers such as carbon nanotubes (CNT) or cellulose nanofibrils (NFC). Unfortunately, compared to standard Newtonian polymer matrices, the impregnation of these polymer suspensions are much more difficult to achieve and to control, as they exhibit highly non-Newtonian properties with shear thinning, yield stress, thixotropic and anisotropic behaviours, resulting in

complex permeation and impregnation mechanisms [6, 7]. Consequently, the impregnation of the fibre reinforcement by the polymer is often uncomplete and leads to the presence of undesirable residual pores altering the composite properties and durability. It also leads to heterogeneities in the fibrous reinforcement.

Most of the theoretical and experimental studies concerning the characterisation of the impregnation process of these materials are performed at a mesoscopic scale, i.e., the scale of an assembly of several fibre bundles or at a macroscopic scale, i.e., the scale of a part. For instance, the permeability of fibrous reinforcement media and the evolution of the flow front is studied using 2D optical visualisation techniques. Few studies focused on the analysis of the pore scale capillary effects and were done using 2D observations [8, 9], thus restraining the analyses to particular flow situations and to limited geometrical descriptions.

Thus, these techniques cannot reveal: (1) the complex local deformation mechanisms that occur at the fibre scale during the fluid propagation in a 3D anisotropic porous fibrous material due to the effect of the interstitial pressure, (2) the complex geometry of the free surface/flow front, (3) the effect of the capillary forces on the geometry of the flow front. Hence, there is a real need to tackle these problem using 3D observations at the pore scale of the impregnation of fibre reinforcements, following the approach that has been used for geomaterials [10-12].

Thus, in this study, we employed high-resolution X-ray microtomography to perform in situ and real-time impregnation experiments of model fibre bundles using impregnation fluids with various viscous properties and modifying the wettability properties of the model bundles. The aim of this work was to give a precise description of the evolving flow front within the model fibre bundles, reproducing phenomena that can occur during the impregnation of fibrous reinforcements.

2. Materials and methods
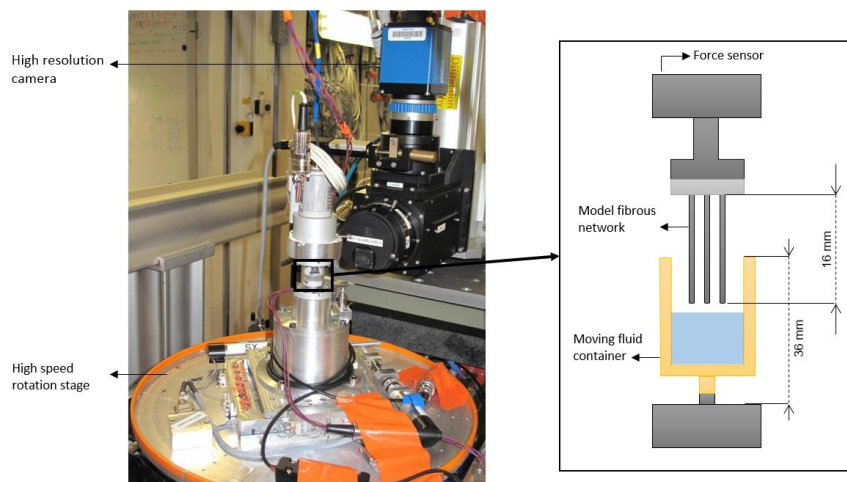
Figure 1. Photograph of the mini impregnation device that was installed on the microtomograph of the ID19 beamline at ESRF (Grenoble, France) and example of two different architectures of the fabricated model bundles of parallel capillary tubes. Note that the tubes were sealed at their upper extremities.

High-resolution X-ray synchrotron microtomography (ID19 beamline at ESRF) was used to perform in situ interrupted impregnation experiments, using a specially designed mini impregnation device (Fig. 1). This imaging technique allowed original 3D observations of impregnation phenomena in

various model bundles to be obtained. In this study different simply-ordered arrangements of parallel capillary tubes were used (Fig. 2). A fluid container was installed on a rotation stage (360°) during images acquisition and was moving up during the experiments so as to impregnate the model fibre bundles. The rigid networks were made of arrangements of parallel tubes made of borosilicate glass 3.3. The tubes had a length of 16 mm and an external diameter of 1.6 mm. For the two studied bundle geometries, the tubes were laid out in two different arrangements, as shown in Figure. 2.
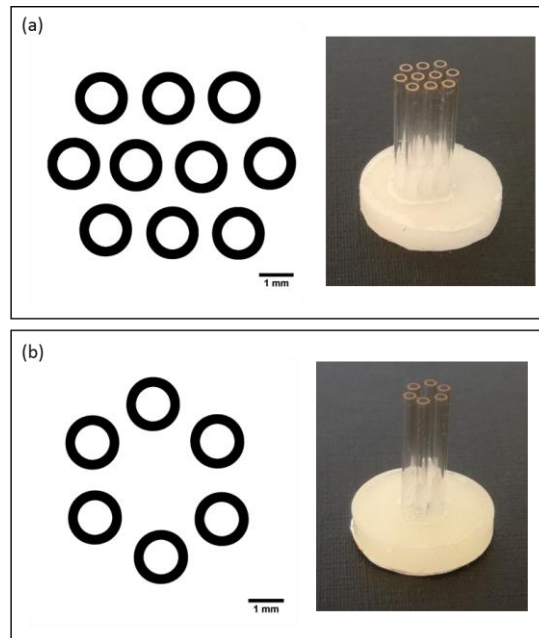
Figure 2. Scheme of the cross sections of the model fibre bundles and photographs of the corresponding samples that were used during the in situ impregnation experiements. (a) 3-4-3 quincux. (b) hexagonal geometry.

To investigate the effect of the wettability properties of the model bundles on the rise of the flow front, the surface properties of the capillary glass tubes (Fig. 2) were modified using chemical vapor-phase silanisation with fluoroalkyl trichlorosilane, the so-called "Si-F treatment". This treatment is known to reduce the wettability of glass [13]. The impregnation experiments were performed using various model fluids with controlled rheological properties and surface tensions: distilled water (γ_L =73 mN m^{-1}, μ = 0.89 mPa·s) and two kinds of silicone oils with close surface tensions but different viscosities (γ_L = 19.9 mN m^{-1}, μ = 20 mPa·s and γ_L =21.1 mN m^{-1}, μ = 1000 mPa·s).

The impregnation was performed plunging the fibre network in the fluid moving at different heights the level of the reservoir. Then, for each height, 3D images of the samples were taken (duration of scan about 1 s). To obtain a good qualtity for the 3D images, 800 radiographs/projections (1584×1584 pixels) of the samples were recorded with a short exposure time (2 ms). Then, 3D images were reconstructed from the radiographies using the phase contrast in the images and the so-called Paganin procedure. For each sample, a sequence of five 3D images of the impregnation process could be obtained with a voxel size of 5.1^3 µm^3 to obtain an accurate representation of the geometry of the free surface of the fluid.

The 3D grey scale images were segmented using software Fiji to distinguish the three phases that form the system: fluid, air and glass tubes (Figs. 3,4). For segmentation, no filters were used in order to avoid modifying the geometry of the fluid-air interface and the triple line between the fluid, tubes and air).

The capillary pressure was computed from the variations in the height using the following expression:

$$\Delta P = P_{cap} = P_{fluid} - P_{air} = \rho g \Delta Z$$

(1)

where ρ and g are the density of the fluid and the gravity force, respectively. Further, the variations in the height ΔZ of the fluid-air interface was measured with respect to a position of the the fluid-air interface where the latter was flat, *i.e.*, far from the meniscus formed by the fluid-air interface in the vicinity of the fibre bundle.

3.Results

Figures 3 and 4 show several images obtained for two different testing conditions: a network of glass tubes with a not treated surface, impregnated with distilled water (Fig. 3) and a network with the same geometry, but where the capillary tubes were subjected to a Si-F treatment to obtain non wetting conditions (Fig. 4). In the first case the distilled water (represented in orange) well impregnated the network of glass tubes. The shape of the fluid front showed a capillary rise higher in the centre of the sample with a dome shape. As the tubes were sealed at their extremities, the distilled water could not rise in the tubes and a meniscus formed at their bottom (Fig. 3d). Note also that slight height variations of the fluid-air interface could be observed in Fig. 3d due to slight misalignments of the tubes forming the model bundle. In the second case a 3D concave surface of the fluid front was observed (Fig. 4) and the inner volume of the network was not impregnated, due to poor wettability of the tubes. Note also the inverse shape of the meniscus formed at the bottom of the capillary tubes, showing that the Si-F treatement was also effective inside the tubes.
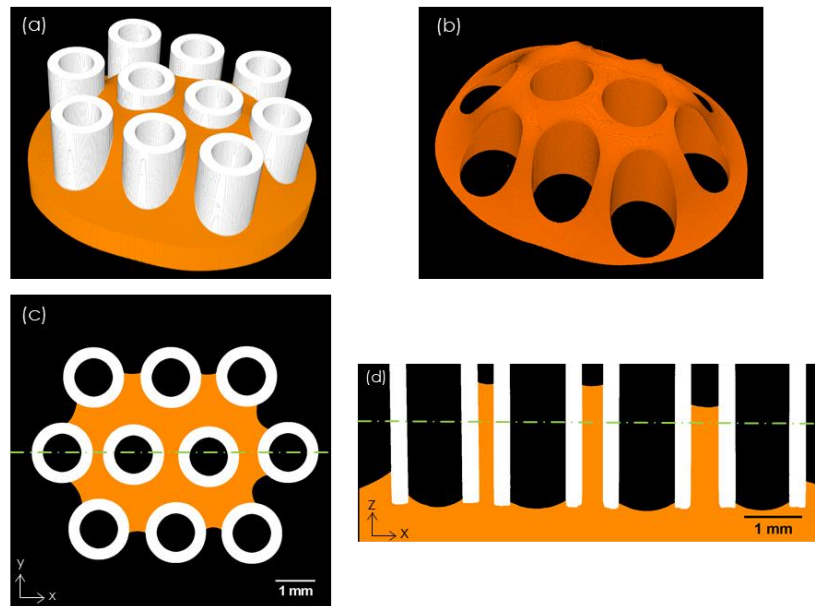
Figure 3. (a) 3D view of a model network made of capillary tubes (white) impregnated with distilled water (orange) obtained using X-ray microtomography imaging (voxel size of 5.1^3 μm^3). (b) Corresponding 3D view of the flow front between the capillary tubes. (c,d) Corresponding horizontal and vertical cross sections. Case of non-treated tubes.
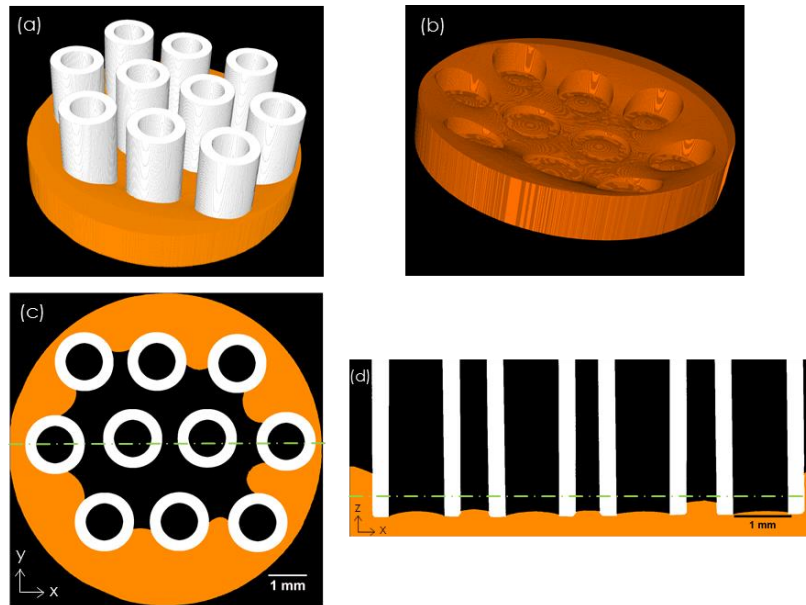
Figure 4. (a) 3D view of a model network made of capillary tubes (white) impregnated with distilled water (orange) obtained using X-ray microtomography imaging (voxel size of 5.1^3 µm^3). (b) Corresponding 3D view of the flow front between the capillary tubes. (c,d) Corresponding horizontal and vertical cross sections. Case of Si-F treated capillary tubes.

Figure 5 shows the variations of the capillary pressure measured at the fluid-air interface for the case shown in Figure 3. The increase in the capillary pressure was the highest in the centre of the fibre bundle, i.e., where the fibre volume fraction was also the highest. Note that the slight misalignement of capillary tubes was accompanied with slight variations of the capillary pressure, thereby showing that within a fibre bundle any structural variations such as fibre volume fraction, fibre misorientation, can result in perturbation of the flow front due to capillary effects.
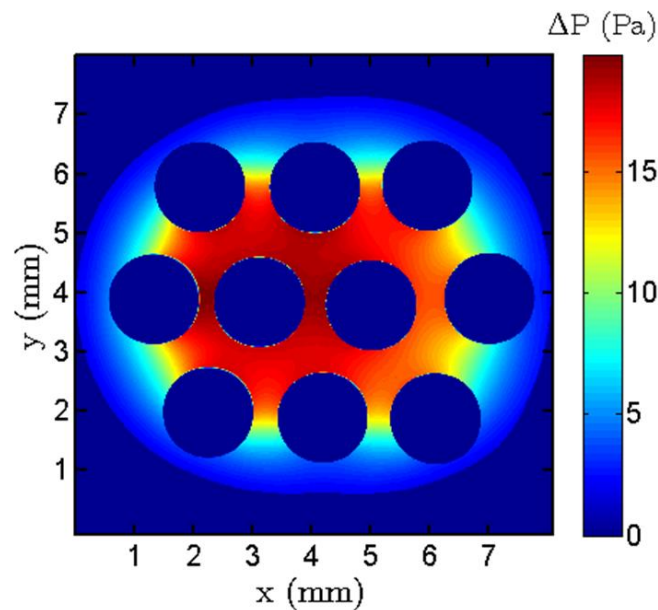
Figure 5. Capillary pressure map onto the fluid-air interface measured for the 3-4-3 quincux arrangement for the case shown in Figure 3.

C. Balbinot et al.

4. Conclusion

This work shows that synchrotron X-ray microtomography is a suitable and efficient tool to enhance the description of impregnation phenomena, in three dimensions, at the fibre pore scale within model fibre bundles. Through the 3D images obtained it was possible to analyse the evolution of the position an geometry of the flow front and to compute the capillary pressure. The effect of various parameters on the impregnation phenomena was studied using this technique. For instance, defects in the architecture of bundles and wettability variations induced by different surfaces treatments were shown to have a great effect of the fluid rise. A deep knowledge of the fluid front evolution at the fibre pore scale is essential to integrate it in macroscale impregnation constitutive models so that the flow front can be described with a more precise geometry than in the actual approaches.

Acknowledgments

References

[1]   E.M. Sozer, P. Simacek, S.G. Advani. Resin transfer molding (RTM) in polymer matrix composites . In Manufacturing Techniques for Polymer Matrix Composites (PMCs). (2012): 245–309.Woodhead Publishing Series in Composites Science and Engineering. https://doi.org/10.1533/9780857096258.3.243

[2]   V.Michaud. A review of non-saturated resin flow in liquid composite moulding processes. *Transport Porous Med.* 115.3 (2016): 581-601.

[3]   L. Orgéas, P.J.J. Dumont, Sheet Molding Compounds, Chapter in Wiley Encyclopedia of Composites, 2nd Edition, Eds. L. Nicolais, A. Borzacchiello, S. M. Lee, ISBN: 978-0-470-12828-2, Wiley, pp. 2683-2718, 2012.

[4]   D. Ferré Sentis, L. Orgéas, P.J.J. Dumont, S. Rolland du Roscoat, M. Sager, P. Latil. 3D in situ observations of the compressibility and pore transport in Sheet Moulding Compounds during the early stages of compression moulding. *Composites Part A* 92 (2017) 51-61.

[5]   D.U. Shah. Developing plant fibre composites for structural applications by optimising composite parameters: a critical review. *J. Mater. Sci.* 48 (2013) 6083-6107.

[6]   Z Idris, L. Orgéas, C. Geindreau, J.-F. Bloch, J.-L. Auriault. Microstructural effects on the flow law of power-law fluids through fibrous media. *Modelling Simul. Mater. Sci. Eng.* 12 (2004) 995-1015.

[7]   T. Chevalier, L. Talon. Generalization of Darcy's law for Bingham fluids in porous media: From flow-field statistics to the flow-rate regimes. *Phys. Rev. E* 91 (2015) 023011.

[8]   Y.-T. Chen, H. T. Davis, C. W. Macosko. Wetting of fiber mats for composites manufacturing: I. Visualization experiments. *AIChE Journal*, 41 (1995) 2261-2273.

[9]   M.A.B. Abdelwahed et al. Bubble formation and transport in T-junction for application to Liquid Composite Molding: Wetting effect. *J. Compos. Mater.* 48.1 (2014): 37-48.

[10] M.Andrew et al. The imaging of dynamic multiphase fluid flow using synchrotron-based X-ray microtomography at reservoir conditions. *Transport Porous Med.* 110 (2015): 1-24.

[11] R.T. Armstrong, M. L. Porter, and D. Wildenschild. Linking pore-scale interfacial curvature to column-scale capillary pressure. *Adv. Water Resour.* 46 (2012): 55-62.

[12] A.Scanziani , et al. Automatic method for estimation of in situ effective contact angle from X-ray micro tomography images of two-phase flow in porous media. *J. Colloid Interface Sci.* 496 (2017): 51-59.

[13] M. Psarski, G. Celichowski, E. Bystrzycka, D. Pawlak, Jarosł. Grobelny, Michał. Cichomski, Vapor phase deposition of fluoroalkyl trichlorosilanes on silicon and glass: Influence of

deposition conditions and chain length on wettability and adhesion forces, *Mater. Chem. Phys.* (2017): 10.037.

[14] Rohatgi, V., N. Patel, and L. James Lee. Experimental investigation of flow-induced microvoids during impregnation of unidirectional stitched fiberglass mat. *Polym. Composite* 17 (1996): 161-170.

[15] J. Bico, B. Roman, L. Moulin, A. Boudaoud, Elastocapillary coalescence in wet hair. *Nature* 432 (2004): 690-690.